Mechanism of action of *N*-acyl and *N*-alkoxy fosmidomycin analogs: mono- and bisubstrate inhibition of IspC from *Plasmodium falciparum*, a causative agent of malaria.

Misgina B. Girma[†], Haley S. Ball[†], Xu Wang[≠], Robert C. Brothers[‡], Emily R. Jackson[‡], Marvin J. Meyers[Δ], Cynthia S. Dowd[‡], Robin D. Couch[*, †].

[†]Department of Chemistry and Biochemistry, George Mason University, Manassas, VA 20110, United States of America. [≠]Progenra Inc, Malvern, PA 19355, United States of America. [Δ]Department of Chemistry, Saint Louis University, Saint Louis, MO 63103, United States of America. [‡]Department of Chemistry, The George Washington University, Washington, DC 20052, United States of America.

TABLE OF CONTENTS

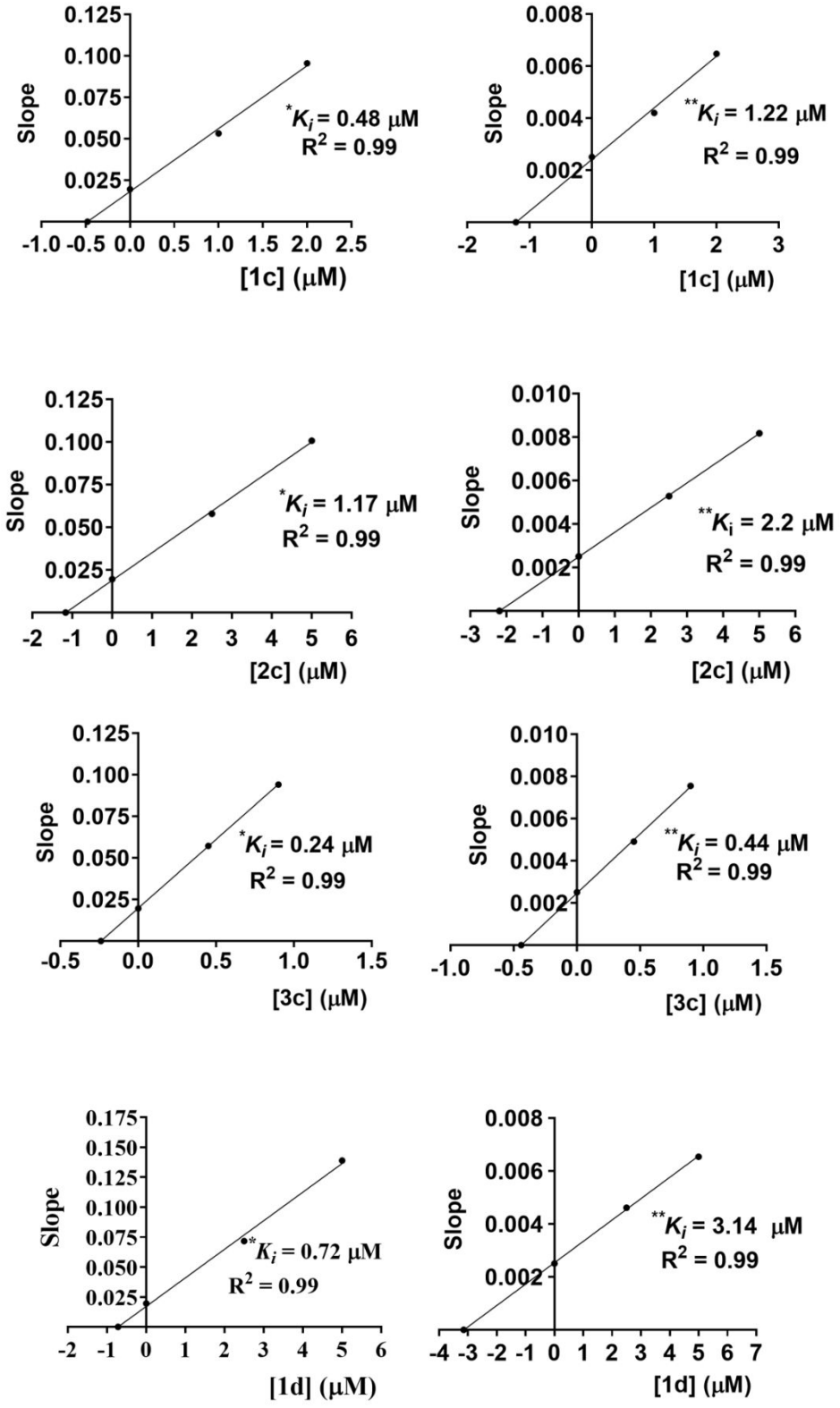

Figure S1. Inhibition constant (K_i) values of *N*-alkoxy fosmodomycin analogs: **1c**, **2c**, **3c**, and **1d**. * = Against the DXP-binding pocket of *P. falciparum* IspC; ** = Against the NADPH-binding pocket of *P. falciparum* IspC. All *N*-alkoxy fosmidomycin analogs showed

a competitive mode of inhibition against both the DXP- and NADPH-binding pockets. The K_i value was determined by generating a secondary plot of the slope of the corresponding Lineweaver-Burk plot as a function of inhibitor concentration. To determine the MoI with respect to the DXP-binding site, the DXP concentration was varied between 50-400 μM while the NADPH concentration was kept constant at 150 μM. To determine the MoI with respect to the NADPH-binding site, the NADPH concentration was varied between 6-30 μM while the DXP concentration was kept constant at 144 μM. All the MOI assays were performed at least in triplicate.

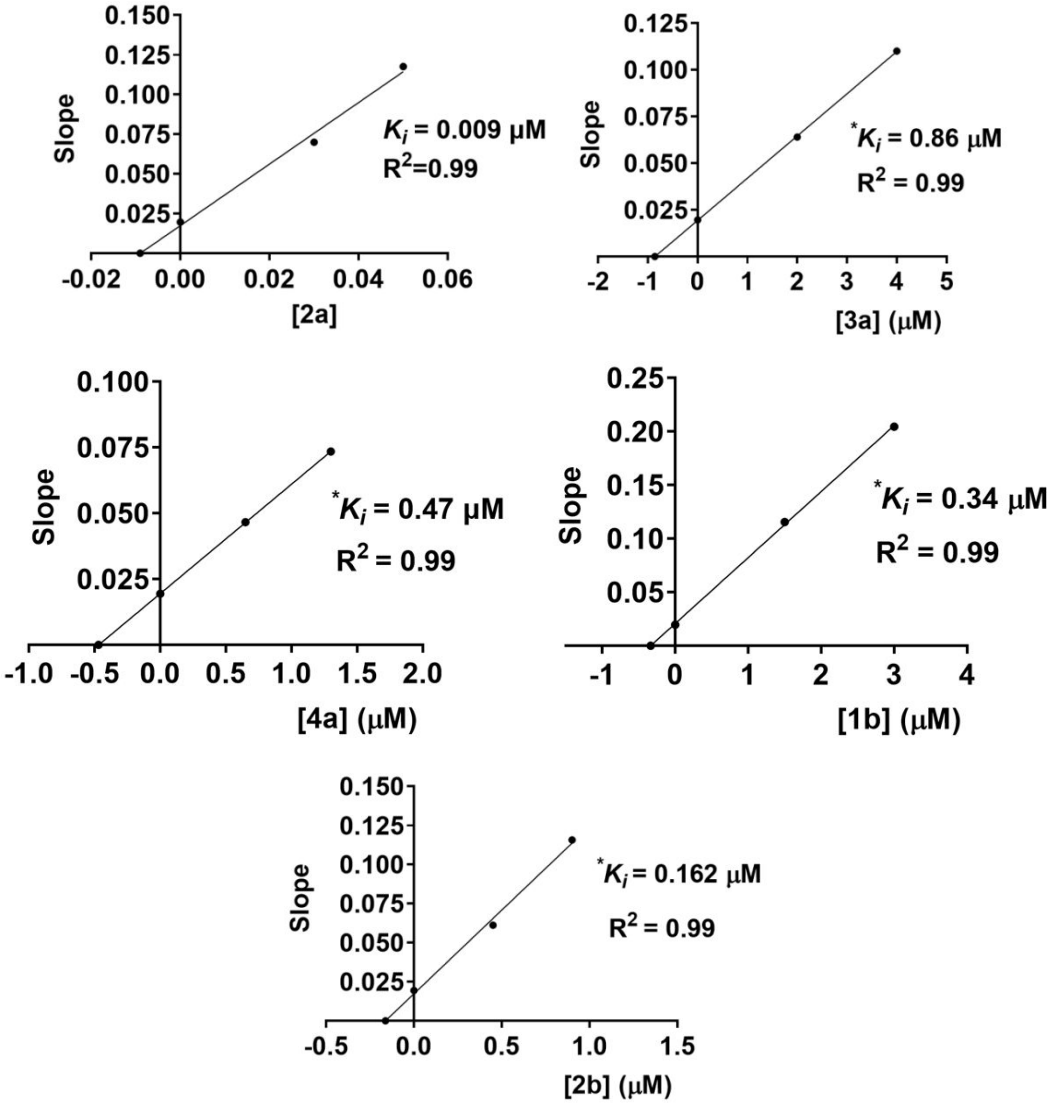

Figure S2. Inhibition constant (K_i) values of saturated *N*-acyl fosmidomycin analogs **2a** = FR900098, **3a**, **4a,** and unsaturated *N*-acyl fosmidomycin analogs **1b** and **2b**. * = Against the DXP-binding pocket of *P. falciparum* IspC. All *N*-acyl fosmidomycin analogs showed a competitive mode of inhibition against the DXP-binding pocket and an uncompetitive mode of inhibition with respect to the NADPH-binding pocket. The K_i value with respect

to the DXP-binding pocket was determined by generating a secondary plot of the slope of the corresponding Lineweaver-Burk plot as a function of inhibitor concentration. To determine the MoI with respect to the DXP-binding site, the DXP concentration was varied between 50-400 μM while the NADPH concentration was kept constant at 150 μM. To determine the MoI with respect to the NADPH-binding site, the NADPH concentration was varied between 6-30 μM while the DXP concentration was kept constant at 144 μM. All the MOI assays were performed at least in triplicate.

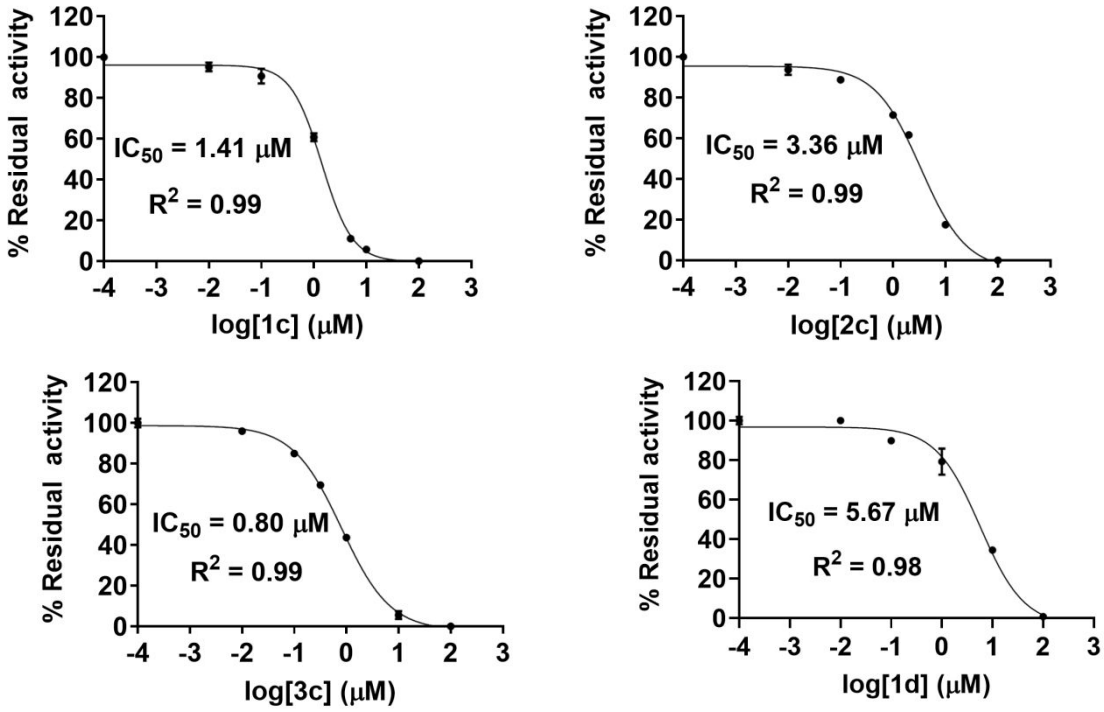

Figure S3. Half-maximal inhibitory concentrations (IC_{50}) of *N*-alkoxy fosmidomycin analogs **1c**, **2c**, **3c** and **1d** against the activity of *P. falciparum* IspC. All the assays required to determine the IC_{50}s were performed in duplicate, and the curve fitting was executed by plotting both data points at each concentrations of the inhibitor.

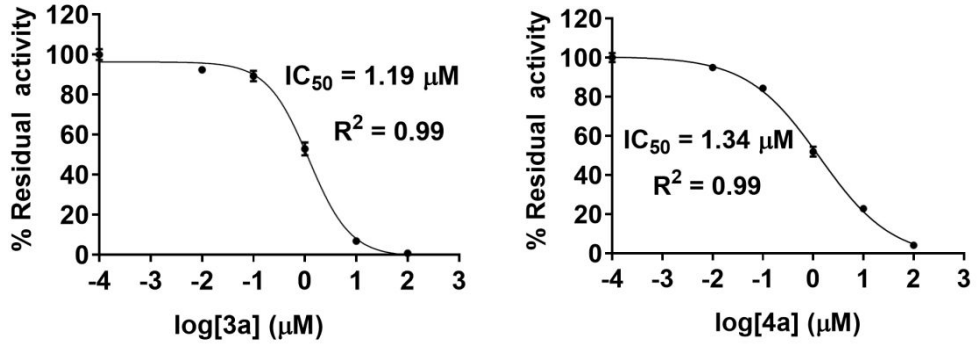

Figure S4. Half-maximal inhibitory concentrations (IC_{50}) of saturated *N*-acyl fosmidomycin analogs **3a** and **4a** against the activity of *P. falciparum* IspC. The IC_{50} of compounds **1a** and **2a** were reported previously[1]. All the assays required to determine the IC_{50}s were performed in duplicate, and the curve fitting was executed by plotting both data points at each concentrations of the inhibitor.

[1]Xu Wang, Rachel L. Edwards, Haley Ball, Claire Johnson, Amanda Haymond, Misgina Girma, Michelle Manikkam, Robert C. Brothers, Kyle T. McKay, Stacy D. Arnett, Damon M. Osbourn, Sophie Alvarez, Helena I. Boshoff, Marvin J. Meyers, Robin D. Couch, Audrey R.Odom John, Cynthia S. Dowd. *J Med Chem.* 2018, **61**(19), 8847–8858.

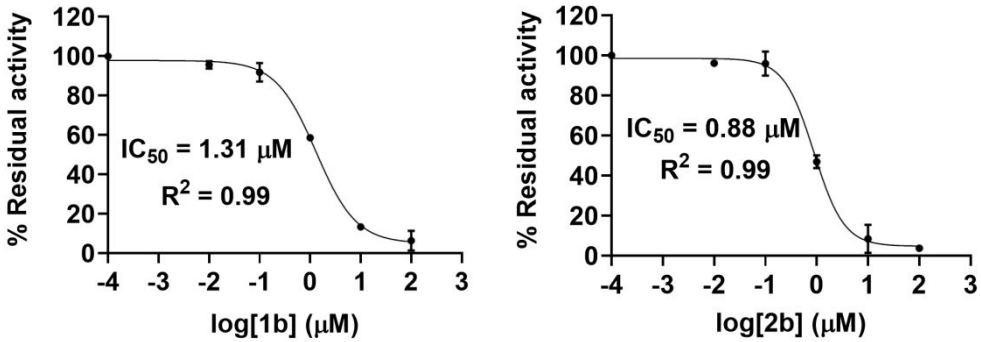

Figure S5. Half-maximal inhibitory concentrations (IC_{50}) of *α,β*-unsaturated *N*-acyl fosmidomycin analogs **1b** and **2b** against the activity of *P. falciparum* IspC. All the assays required to determine the IC_{50}s were performed in duplicate, and the curve fitting was executed by plotting both data points at each concentrations of the inhibitor.

Table S1. *P. falciparum* structures used in the molecular modeling studies.

Reference	PDB	Ligand	NADPH present in crystal structure?	Trp296 position relative to 3AUA	His293 position relative to 3AUA
Umeda et al. (2015)	3AUA	FR900098	yes	-	-
Konzuch et al. (2014)	3WQR	*α*-aryl analog	yes	Replaced by His293	Replaced Trp296
Chofor et al. (2015)	4Y67	*β*-$(CH_2)_3$Ph	no	Displaced by Ph of ligand	Shifted away from active site
Chofor et al. (2015)	4Y6R	*β*-Ph	no	No change	Shifted away from active site

Umeda, T.; Tanaka, N.; Kusakabe, Y.; Nakanishi, M.; Kitade, Y.; Nakamura, K. T. Molecular Basis of Fosmidomycin's Action on the Human Malaria Parasite *Plasmodium Falciparum*. *Sci. Rep.* **2011**, *1*,9. https://doi.org/10.1038/srep00009.

Konzuch, S.; Umeda, T.; Held, J.; Hähn, S.; Brücher, K.; Lienau, C.; Behrendt, C. T.; Gräwert, T.; Bacher, A.; Illarionov, B.; Fischer, M.; Mordmüller, B.; Tanaka, N.; Kurz, T. Binding Modes of Reverse Fosmidomycin Analogs toward the Antimalarial Target IspC. J. Med. Chem. 2014, 57 (21), 8827–8838. https://doi.org/10.1021/jm500850y.

Chofor, R.; Sooriyaarachchi, S.; Risseeuw, M. D. P.; Bergfors, T.; Pouyez, J.; Johny, C.; Haymond, A.; Everaert, A.; Dowd, C. S.; Maes, L.; Coenye, T.; Alex, A.; Couch, R. D.; Jones, T. A.; Wouters, J.; Mowbray, S. L.; Van Calenbergh, S. Synthesis and Bioactivity of β-Substituted Fosmidomycin Analogues Targeting 1-Deoxy-d-Xylulose-5-Phosphate Reductoisomerase. *J. Med. Chem.* **2015**, *58* (7), 2988–3001. https://doi.org/10.1021/jm5014264

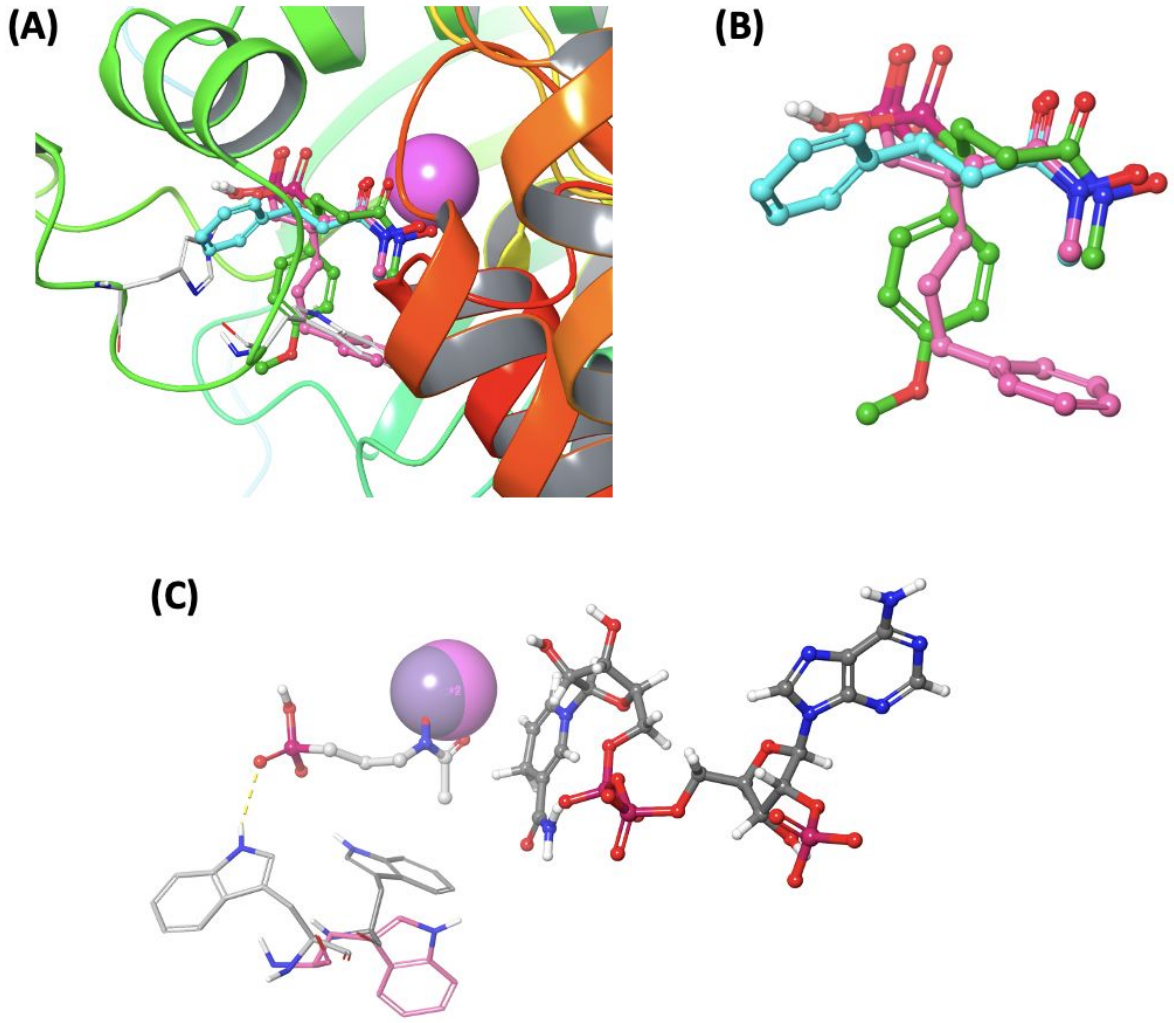

Figure S6. Overlay of crystal structures used in modeling studies showing (A) binding poses of *α*- and *β*-substituted ligands relative to His293 and Trp296 from 3AUA (gray 3AUA; green *α*-aryl analog from 3WQR; cyan *β*-Ph analog from 4Y6R; magenta *β*-$(CH_2)_3$Ph analog from 4Y67). (B) Protein ribbon removed for clarity. (C) Overlay of 3AUA, 3WQR and 4Y67 illustrating alternative positions of Trp296.

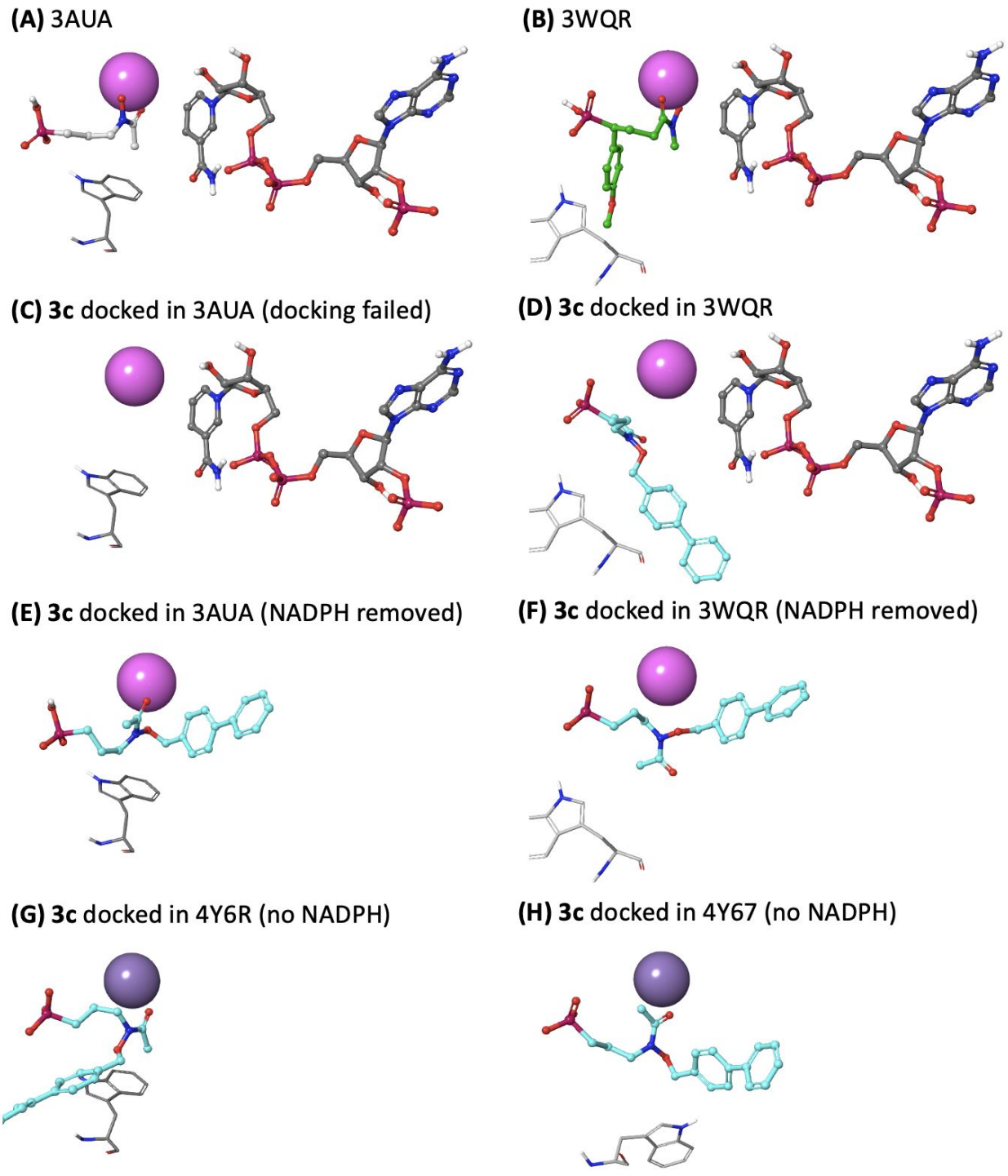

Figure S7 Reference structures: (A) 3AUA crystal structure showing DXP, NADPH, Mg^{2+}, and Trp296 and (B) 3WQR crystal structure showing *α*-aryl analog, NADPH, Mg^{2+}, and Trp296. Docking studies with *N*-alkoxy compound **3c**: (C) docking failed in 3AUA in the presence of NADPH; (D) docking in 3WQR in the presence of NADPH produced a structure that failed to produce a bidentate binding pose with Mg^{2+}; (E) docking in 3AUA in the absence of NADPH produced a structure that did produce a bidentate binding pose

with Mg^{2+}; (F) docking in 3WQR in the absence of NADPH produced a structure that failed to produce a bidentate binding pose with Mg^{2+}; (G) docking in 4Y6R produced a structure that failed to produce a bidentate binding pose with Mg^{2+}; (H) docking in 4Y67 produced a structure that failed to produce a bidentate binding pose with Mg^{2+}.

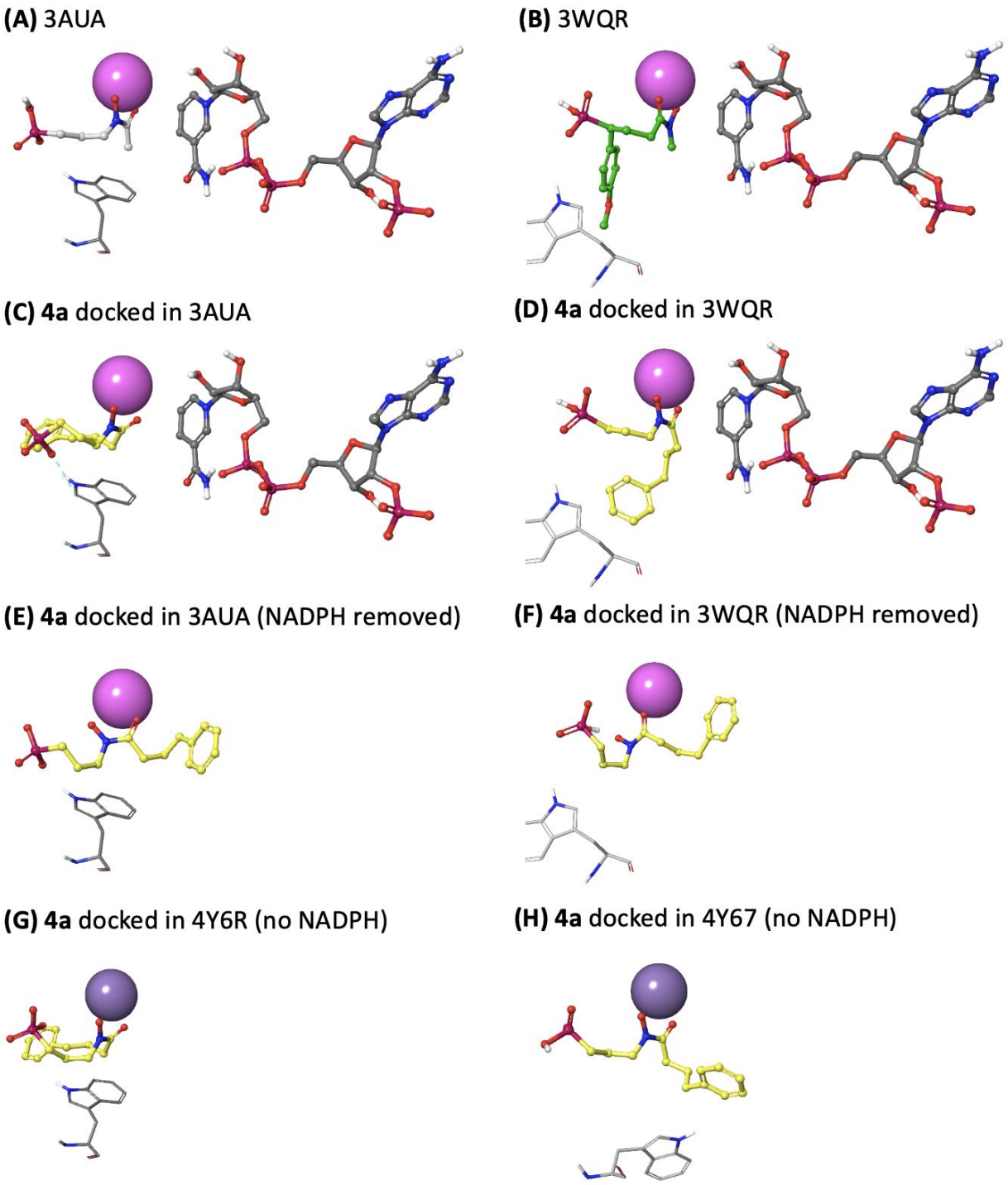

Figure S8. Reference structures: (A) 3AUA crystal structure showing DXP, NADPH, Mg^{2+}, and Trp296 and (B) 3WQR crystal structure showing *α*-aryl analog, NADPH, Mg^{2+}, and Trp296. Docking studies with *N*-acyl compound **4a**: (C) docking in 3AUA in the presence of NADPH produced a bidentate binding pose with Mg^{2+}; (D) docking in 3WQR in the presence of NADPH produced a structure produced a bidentate binding pose with Mg^{2+}; (E) docking in 3AUA in the absence of NADPH produced a bidentate binding pose

with Mg^{2+}; (F) docking in 3WQR in the absence of NADPH produced a structure that failed to produce a bidentate binding pose with Mg^{2+}; (G) docking in 4Y6R produced a structure that produced a bidentate binding pose with Mg^{2+}; (H) docking in 4Y67 produced a structure that produced a bidentate binding pose with Mg^{2+}.

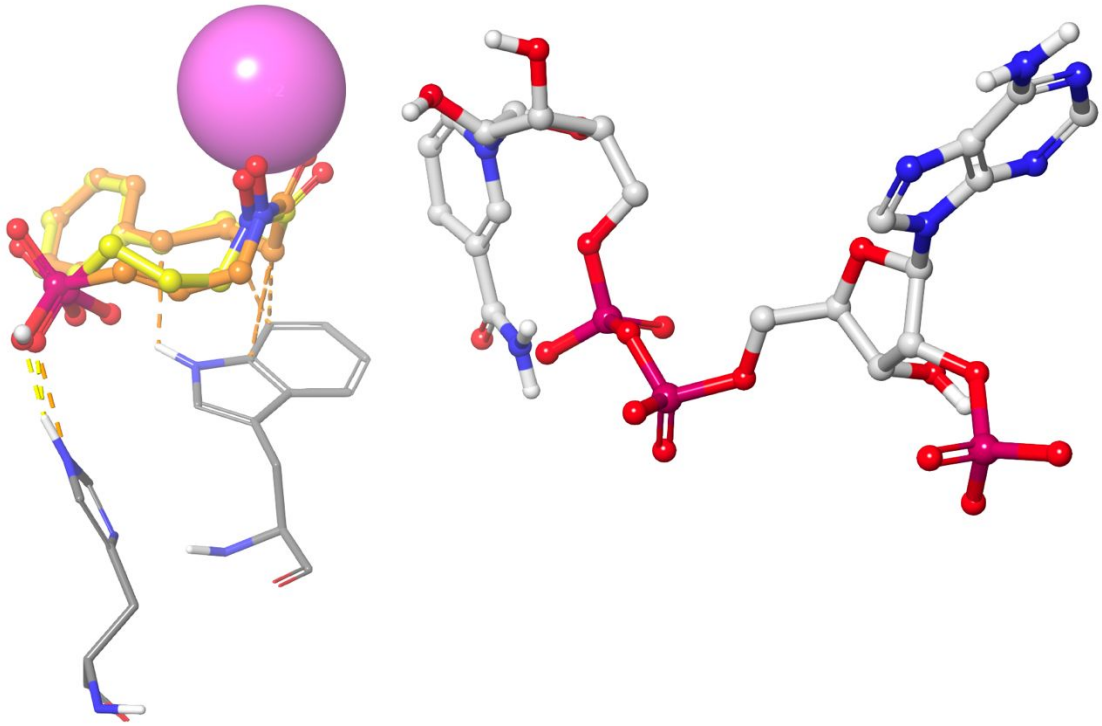

Figure S9. Overlay of docked *N*-acyl fosmidomycin analogs 4a and 2b. *N*-acyl analogs **4a** and **2b** were docked in *P. falciparum* IspC/FR900098 structure 3AUA with NADPH present. Trp296 and His293 are colored dark gray. NADPH is colored light gray. Mg^{2+} is colored magenta. Docked saturated *N*-acyl analog **4a** is colored yellow. Docked unsaturated *N*-acyl analog **2b** is colored orange.